J. Cent. South Univ. Technol. (2011) 18: 1819−1824
DOI: 10.1007/s11771−011−0908−y

Springer

Influence of methane on hot filament CVD diamond films deposited on high-speed steel substrates with WC-Co interlayer

WANG Ling(王玲)[1], WEI Qiu-ping(魏秋平)[1, 2], YU Zhi-ming(余志明)[1, 2], WANG Zhi-hui(王志辉)[1], TIAN Meng-kun(田孟昆)[1]

1. School of Materials Science and Engineering, Central South University, Changsha 410083, China;
2. State Key Laboratory of Powder Metallurgy, Central South University, Changsha 410083, China

Abstract: Diamond films were deposited on high-speed steel substrates by hot filament chemical vapor deposition (HFCVD) method. To minimize the early formation of graphite and to enhance the diamond film adhesion, a WC-Co coating was used as an interlayer on the steel substrates by high velocity oxy-fuel spraying. The effects of methane content on nucleation, quality, residual stress and adhesion of diamond films were investigated. The results indicate that the increasing methane content leads to the increase in nucleation density, residual stress, the degradation of quality and adhesion of diamond films. Diamond films deposited on high-speed steel (HSS) substrate with a WC-Co interlayer exhibit high nucleation density and good adhesion under the condition of the methane content initially set to be a higher value (4%, volume fraction) for 30 min, and then reduced to 2% for subsequent growth at pressure of 3 kPa and substrate temperature of 800 °C.

Key words: diamond film; WC-Co interlayer; methane; nucleation density; adhesion

1 Introduction

Chemical vapor deposition (CVD) diamond coatings have enormous technological potential due to their exceptional mechanical and physical properties such as the highest hardness, high thermal conductivity, chemical inertness and wear resistance [1−2]. Many kinds of steels are widely used for the manufacture of wear resistant components and cutting tools, so well-adhered diamond films deposited on steel surfaces can offer an opportunity to enhance the resistance of steel to wear and corrosion, but also retain the mechanical properties of steel. Hence, diamond coated steel has obvious attractive commercial potential [3−4]. However, direct deposition of CVD diamond on steel substrates is extremely difficult due to the following obstacles [5−7]: 1) the diffusion of carbon into steel at high temperatures during CVD process leads to very low nucleation density, the formation of cementites (e.g. Fe_3C) and interfacial graphite and the degradation of the microstructure and properties of the steel; 2) iron has a catalytic effect on the growth of sp^2 dominated amorphous and nanocrystalline carbon, therefore, in many cases, diamond films are actually grown on a layer of soft graphite instead of carburized iron; 3) the large difference in thermal expansion coefficients between diamond and steel ($\alpha_{diamond}=1\times10^{-6}\,K^{-1}$, $\alpha_{HSS}=11\times10^{-6}\,K^{-1}$ at room temperature [8]) may induce high residual stress within diamond films.

A solution to these problems is the use of an interlayer system between the steel substrate and the diamond coating. In principle, the selected interlayer should meet the following requirements [9]: 1) avoid the diffusion of Fe towards interlayer surface; 2) allow the nucleation and growth of diamond on interlayer surface; 3) supply a good bonding to both diamond films and steel substrate; 4) have a suitable thermal expansion coefficient, which should be beneficial in reducing the mismatch between diamond and substrate. Improved nucleation and adhesion of diamond films have been obtained by the applications of various interlayers, such as W [8], Al [10], Mo [11], Ti, Cr [12], TiC [13] and CrN [1].

The hot filament (HF) assisted CVD methods of adherent diamond films on carbon steel substrates that had themselves been pre-coated with a thin WC-Co interlayer have been reported recently [14−15]. Successful diamond growth was achieved after pre-treating the WC-Co interlayer with a two stage etching process,

Foundation item: Project(1343-74236000005) supported by the Innovation Foundation for Postgraduates of Hunan Province, China; Project(ZKJ2008001) supported by the Open Fund for Valuable Instruments of Central South University, China; Project(2008112048) supported by the Open Fund of State Key Laboratory of Metallurgy, China
Received date: 2010−09−16; **Accepted date**: 2010−12−16
Corresponding author: WEI Qiu-ping, Professor, PhD; Tel: +86−731−88830335; E-mail: qiupwei@csu.edu.cn

which had the effect of depleting the Co content on the surface. A range of pretreatment methods for diamond films deposited on sintered WC-Co substrates with different cobalt contents have also been investigated [16−18]. This work reports more extensive investigations of HFCVD of diamond films on another kind of steel substrate (i.e. high-speed steel) with a thinner WC-Co interlayer. By optimizating the CVD processing parameters, a significant enhancement in the adhesion of diamond film and an obvious improvement of the crystalline quality were achieved.

2 Experimental

Polished plates of high-speed steel $W_{18}Cr_4V$ (0.79% C, 0.21% Si, 0.15% Mn, 18.65% W, 4.2% Cr, 1.16% V, 0.11% Mo, in mass fraction) with dimensions of 10 mm× 8 mm × 2 mm were used as substrates. The steel plates were covered with a WC-Co interlayer (~50 μm in thickness) by high velocity oxygen fuel (HVOF) thermal spray process. The WC-Co blends used here typically comprised 85%−90% WC and 10%−15% Co powder (mass fraction, powder size 2−5 μm). The specimens were then etched using the following two-step pretreatment [14−15]: 1) etching by Murakami's reagent (10 g $K_3[Fe(CN)_6]$ + 10 g KOH + 100 mL H_2O) for 3 min in an ultrasonic vessel; 2) removal of the surface Co by etching the specimens in an acidic solution of hydrogen peroxide (2 mL 96% H_2SO_4 + 2 mL 68% HNO_3+20 mL 40% H_2O_2+40 mL H_2O, volume fraction) for 2 min. Finally, the substrate with the interlayer was pre-treated ultrasonically in a suspension of ultrafine (particle size <5 μm) diamond powder to enhance the diamond nucleation density. Table 1 shows the CVD processing parameters used, which were typically held constant for each specimen and deposition. In particular, the specimen D was deposited with the methane content of 4% during nucleation for 0.5 h and 2% during growth for 1.5 h.

Table 1 Experimental parameters used for diamond film deposition on HSS substrates with WC-Co interlayer

Specimen	($V(CH_4)$/ $V(H_2)$)/ %	Substrate temperature/ °C	Deposition pressure/ kPa	Filament-substrate distance/ mm	Deposition time/ h
A	2	800	3	8±2	2
B	3	800	3	8±2	2
C	4	800	3	8±2	2
D	4(0.5 h) 2(1.5 h)	800	3	8±2	2

Specimens were characterized by a variety of techniques, including scanning electron microscopy (FEI, Sirion200 Field-emission SEM and Quanta200 Environmental SEM), X-ray diffraction (Dmax-2500VBX using Cu K_α radiation at a wave length of 0.154 nm) and Raman spectroscopy (LabRAM HR800). Raman spectra were measured with an argon ion laser operating at 488 nm with an output power of 100 mW. The adhesion of the diamond-coated steel substrates was characterized using a Rockwell hardness tester with a cone-shaped diamond indenter of 120°. The diamond-coated surface was indented at loads of 1 000 N and 1 500 N.

3 Results and discussion

Figure 1 shows the cross-section SEM image of a WC-Co interlayer deposited on high-speed steel substrate. It clearly shows a continuous two-layer structure with a ~50 μm-thick WC-Co interlayer on the surface.

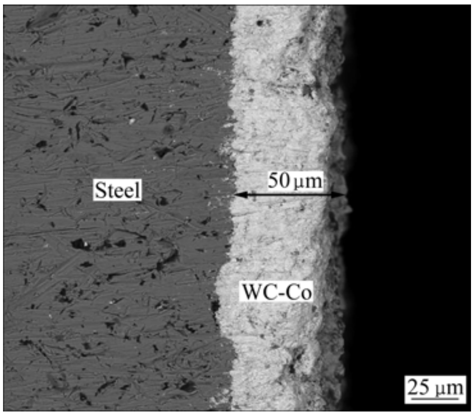

Fig.1 Cross-section SEM image of WC-Co interlayer on HSS substrate

3.1 X-ray diffraction

XRD patterns of the high-speed steel, as-coated WC-Co interlayer deposited on a high-speed steel substrate and CVD diamond film on specimen C, are shown in Figs.2(a), (b) and (c), respectively. Figure 2(a) shows that the dominate phase of high-speed steel is

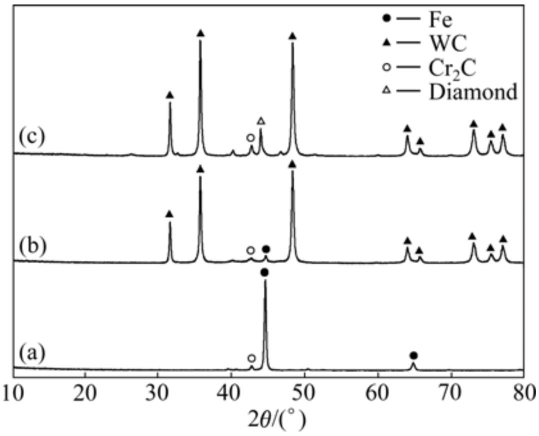

Fig.2 XRD patterns of steel substrate (a), WC-Co interlayer (b) and diamond film on specimen C (c)

elemental iron, while there is also a small amount of Cr_2C. The surface of the as-coated WC-Co interlayer on the high-speed steel substrate (Fig.2(b)) mainly comprises WC and a trace amount of Fe and Cr_2C, no elemental Co is found. The results demonstrate that the two-step pretreatment has a considerable influence in terms of removing Co. The XRD pattern of Fig.2(c) indicates the presence of diamond. Peaks at 2θ diffraction angles of 43.9° and 75.3° are clearly evident. Note that the peak in the range $2\theta\approx75.4°$ matches closely with the diamond (220) peak at 75.302° and the WC (200) peak at 75.477° [18]. Therefore this peak is assigned to the overlapping of diamond (220) and WC (200) peaks.

3.2 Investigation of surface morphology

Figure 3 shows the surface SEM images of diamond films deposited on specimens A−D. The surface images of specimen A reveal that the nucleation density is very low, but the individual crystallites show typical diamond crystal morphologies (see Figs.3(a) and (b)). Both the grain size and the nucleation density of diamond film on specimen B are larger than those of specimen A, but the diamond film nucleates very non-uniformly, furthermore, multi-fold twinned diamond structures can be observed in the film (see Figs.3(c) and (d)). Both specimens C and D show a dense and homogeneous diamond film. In contrary to specimen C, the film on D has a higher

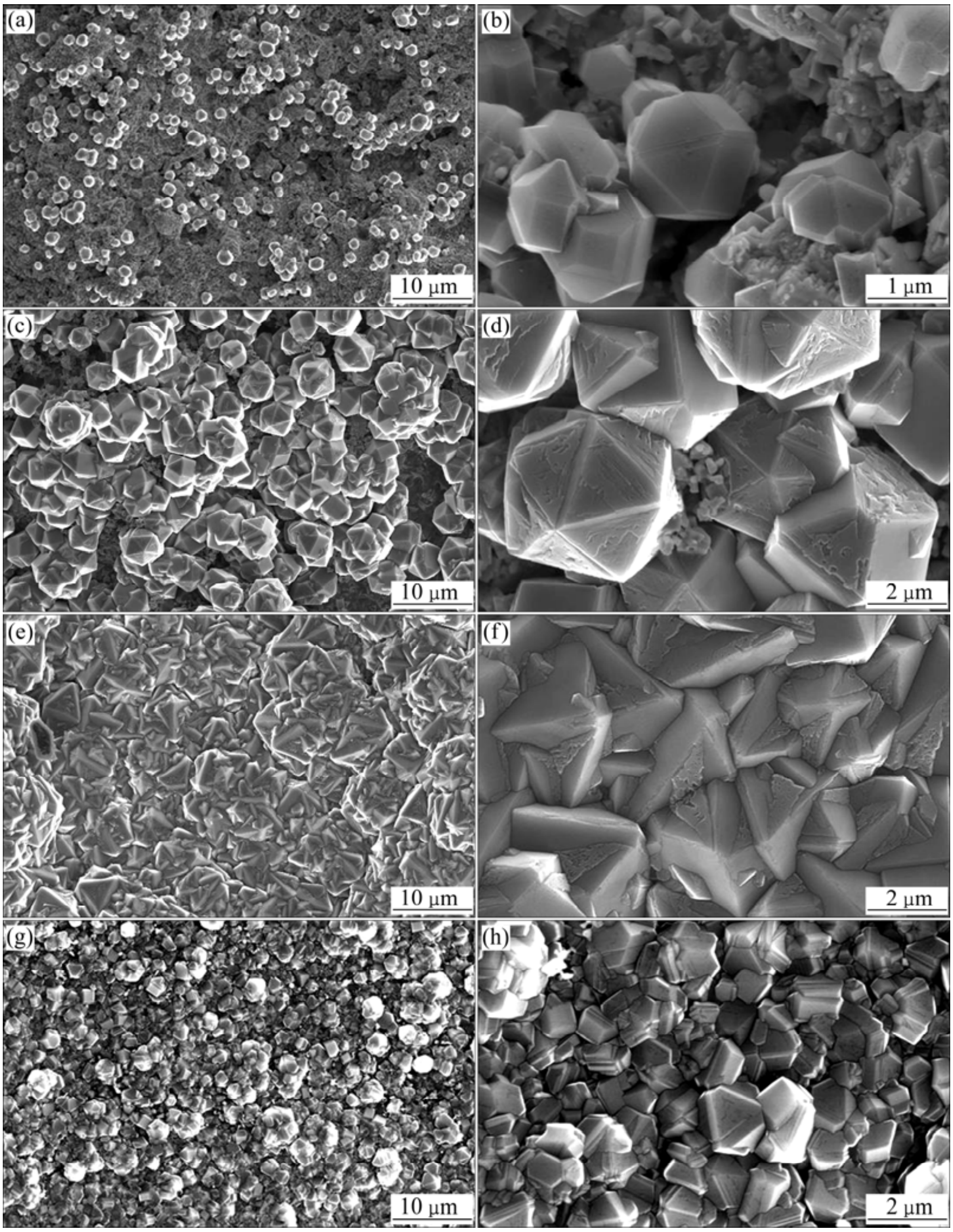

Fig.3 Representative SEM images of diamond films deposited on specimens A (a, b), B (c, d), C (e, f) and D (g, h) (Right SEM images are part of each sample recorded at higher magnification)

diamond nucleation density and a smaller grain size (see Figs.3(e), (f), (g) and (h)).

From the SEM micrographs of Fig.3, it can be concluded that a dramatical increase of nucleation density is achieved with increasing the methane content, because of the increase in the amount of the CH_x species (x=0−3) content [19]. MAY et al [20] have previously argued for a correlation between the [H]/[CH_x] ratio and the resulting CVD diamond film properties, but any such correlation in the present case is likely to be reduced by the variation in substrate temperature within each sample. At low methane content, the increase of the ratio of [H]/[CH_3] will improve the quality of diamond film (as judged by diamond carbon phase purity), but will decrease the growth rate and nucleation rate. It is well known that increasing the methane content leads to an increase in overall nucleation density at the price of degrading film quality [14]. For specimen D, methane is first introduced into the CVD reactor at a relatively high $V(CH_4)/V(H_2)$ ratio (4%) for 30 min, then lowered to 2% for another 90 min. Since the initial $V(CH_4)/V(H_2)$ ratio is the same as specimen C at a high level of 4%, the initial nucleation in both specimens C and D is similar and high. In the second stage of specimen D, however, when the $V(CH_4)/V(H_2)$ ratio is reduced, the diamond crystals grow with better quality.

Especially to be mentioned, when methane content is 3% (Fig.3(d)), the (100) face is smooth while (111) face is rough. These results can be explained by a new growth operating mechanism of stress relaxation induced growth. Continued operation of this growth process could increase the ⟨111⟩ growth rate but apparently decrease that of ⟨100⟩ [21].

3.3 Laser Raman analysis

In order to compare the quality of the diamonds grown at different conditions, micro Raman spectroscopy was applied. Figure 4 shows the Raman spectra for the films deposited on specimens A, B, C and D, respectively. With increasing the methane contents the diamond band, normally positioned at 1 332 cm^{-1}, shifts slightly to higher wavenumber. Significant peaks at ~1 350 cm^{-1} (D band) and ~1 550 cm^{-1} (G band) are both the traditional diagnostic for the presence of sp^2 carbon, which are assigned to disordered vibrational mode and zone center phonons of E_{2g} symmetry of graphite [22−23].

It is well known that great mismatch in thermal expansion for steel (11×10^{-6} K^{-1}) and diamond (1×10^{-6} K^{-1}) causes high compressive stress in the diamond film after deposition. The residual stress can be calculated theoretically by the coefficients of thermal expansion.

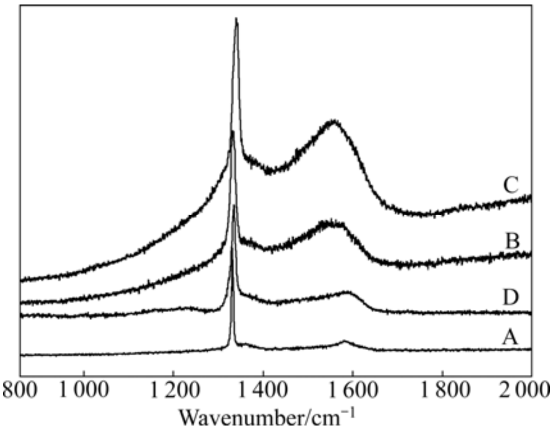

Fig.4 Raman spectra of diamond films deposited on specimens A, B, C and D

The thermal stress (σ_{th}) of a thin diamond layer on top of a thick substrate can be approximated by [24]

$$\sigma_{th} = \frac{E}{1-\nu}\int_{T_{room}}^{T_2}[\alpha_s(T)-\alpha_f(T)]dT \quad (1)$$

where E=1 143 GPa and ν=0.07 are elastic modulus and Poisson ratio for diamond, averaged over different crystallite orientations; α_f and α_s are the temperature-dependent coefficients of thermal expansion of diamond film and steel, respectively, and T_2≈800 °C is the deposition temperature. For diamond, the value of α_f increases from 1×10^{-6} K^{-1} at room temperature to 4.5×10^{-6} K^{-1} at 800 °C, while α_s for steel changes in a minor extent from 11.0×10^{-6} K^{-1} to 13.2×10^{-6} K^{-1} at the same temperature interval [8]. By using Eq.(1), a stress value of 7.2 GPa is obtained. This result can be compared with the value of stress determined from the position of the Raman peak. The residual stress σ is calculated from the measured shift of the diamond peak from the unstressed position at 1 332 cm^{-1} by using the equation (2) [10]:

$$\sigma = -0.567(\nu_c - \nu_0) \quad (2)$$

where ν_0 = 1 332 cm^{-1}; ν_c is the measured position. The experimentally measured data and the theoretically expected values are summarized in Table 2. Obviously, the measured value is always lower than the theoretically expected value. The reduction of residual stress is possible by the WC-Co interlayer. Tungsten carbide has a low thermal expansion coefficient (relative to many other interlayers), the addition content of the cementing metal cobalt will influence the thermal expansion coefficient of WC-Co [25], but it is still lower than that of steel substrates, which should be beneficial in reducing the mismatch between the thermal expansion coefficients of diamond and the substrate (α_{WC}= 4.42×10^{-6} K^{-1} (25−500 °C), α_{Co}=12.5×0^{-6} K^{-1} (0−100 °C)) [26]. Moreover, the volume expansion during cooling also contributes to

Table 2 Residual stress of diamond films and FWHM of sp^3 peaks measured by Raman spectra

Specimen	Calculated σ_{th}/GPa	Measured σ/GPa	FWHM/ cm^{-1}
A	−7.2	0	4.22
B	−7.2	−0.61	13.87
C	−7.2	−4.30	14.43
D	−7.2	−1.10	7.39

the reduction of residual stresses.

From the results, it can be also concluded that the residual stress increases as increasing the methane content. For specimen A, diamond crystallines are randomly scattered without the formation of continuous diamond film, the shrink of steel substrate will not induce compressive stress as the specimen A cooling down from high deposition temperature to room temperature. So the wavenumber center of diamond Raman peak of specimen A is close to the peak position of the natural, stress-free diamond sample (1 332 cm^{-1}). It is found that the residual stress of specimen B is non-uniform according to the Raman spectra recorded several times at different areas, which may be resulted from the non-uniform nucleation of diamond film as shown in Figs.3(c) and (d). Although the films of both specimens C and D are continuous and compact, the residual stress of specimen C is larger than that of specimen D. It is owing to that the grain size of specimen D is smaller than that of specimen C, so the film of specimen D has more grain boundary, which is favorable to the relaxation of stress.

In order to analyze the quality of the diamond films, the full width at half maximum (FWHM) of the sp^3 peaks was measured by Raman spectra. The films with lower FWHM have better crystalline quality, and vice versa. Typical FWHMs of the diamond peak at 1 332 cm^{-1} are listed in Table 2. A significant increase of FWHM with increasing methane content can be observed. It can be explained that at low methane content, the comparative ratio between atomic hydrogen and methyl radical increases with decreasing the methane content. Thus, non-diamond species can be etched off, which is also supported by the SEM micrographs in Fig.3. Furthermore, the FWHMs increase with the increase of residual stress. Because the residual stress in diamond film is anisotropic and nonuniform, it is hypothesized that the large FWHM could be attributable to a wide distribution of stress values in the diamond [27]. So, the higher the residual stress is, the higher the FWHM is.

3.4 Indentation testing

Rockwell indentation was performed with various loads to estimate the adhesion of diamond films on specimens C and D. Since continuous films were not formed on specimens A and B, the residual stress of them was not considered. The results show that large scale flaking-off is evident around both indentations on specimen C (see Figs.5(a) and (b)), but no flaking or cracking is observed around the indentation on specimen D (see Figs.5(c) and (d)), demonstrating the good adhesion of diamond film on specimen D. Such findings are consistent with the residual stress analysis results shown in Table 2.

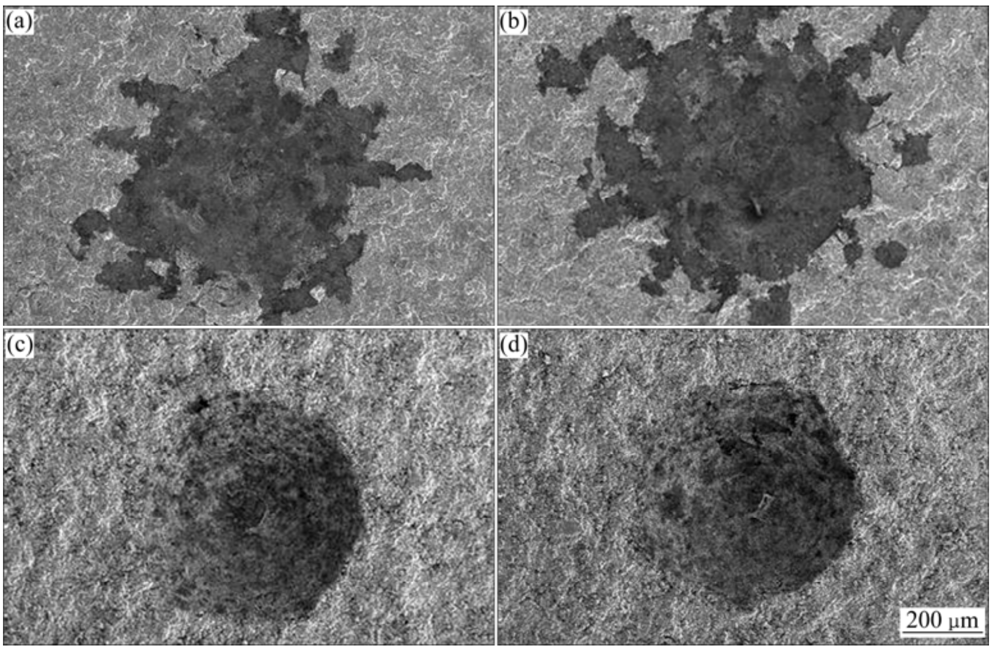

Fig.5 SEM images of Rockwell indentations on specimens C ((a), (b)) and D ((c), (d)) under loads of 1 000 N ((a), (c)) and 1 500 N ((b), (d))

4 Conclusions

1) A Co-containing tungsten-carbide (WC-Co) coating prepared by high velocity oxy-fuel spraying can effectively block the diffusion of Fe and reduce the residual stress of films. Dense and well-adhered diamond films are successfully deposited on high-speed steel substrates with WC-Co interlayer under an appropriate CVD processing condition.

2) The nucleation density, quality, residual stress and adhesion of diamond film strongly depend on the methane content. The nucleation density increases with increasing the methane content, but the quality and adhesion of diamond deteriorate at the same time.

3) Deposition at a higher methane content for nucleation and subsequently at a lower content for growth can not only increase the nucleation density and improve the quality of film, but also reduce the residual stress and obtain a good adhesion, making the technique useful for industrial application. The best diamond film is obtained for high-speed steel substrate under the condition of the methane content initially set to a higher value (4%, volume fraction) for 30 min, and then reduced to 2% for subsequent growth at pressure of 3 kPa and substrate temperature of 800 °C.

References

[1] GLOZMAN O, HALPERIN G, ETSIO I, BERNER A, SHECTMAN D, LEE G H, HOFFMAN A. Study of the wear behavior and adhesion of diamond films deposited on steel substrates by use of a Cr-N interlayer [J]. Diamond and Related Materials, 1999, 8(2/3/4/5): 859−864.

[2] YANG Q, TANG Y, YANG S L, HIROSEB A. Simultaneous growth of diamond thin films and carbon nanotubes at temperatures ≤550 ℃ [J]. Carbon, 2008, 46(4): 589−595.

[3] GOWRI M, LI H, SCHERMER J J, ENCKEVORT W J P, MEULEN J J. Direct deposition of diamond films on steel using a three-step process [J]. Diamond and Related Materials, 2006, 15(4/5/6/7/8): 498−501.

[4] SIKDER A K, MISRA D S, SINGHBAL D, CHAKRAVORTY S. Surface engineering of metal-diamond composite coatings on steel substrates using chemical vapour deposition and electroplating routes [J]. Surface and Coatings Technology, 1999, 114(2/3): 230−234.

[5] NAKAMURA E, HIRAKURI K K, OHYAMA M. High quality chemical vapor deposition diamond growth on iron and stainless steel substrates [J]. Journal of Applied Physic, 2002, 92 (6): 3393−3396.

[6] BORGES C F M, PFENDER E, HEBERLEIN J. Influence of nitrided and carbonitrided interlayers on enhanced nucleation of diamond on stainless steel 304 [J]. Diamond and Related Materials, 2001, 10(11): 1983−1990.

[7] SCHWARZ S, ROSIWAL S M, MUSAYEV Y, SINGER R F. High temperature diffusion chromizing as a successful method for CVD-diamond coating of steel (Part II) [J]. Diamond and Related Materials, 2003, 12(3/4/5/6/7): 701−706.

[8] RALCHENKO V G, SMOLIN A A, PEREVERZEV V G. Diamond deposition on steel with CVD tungsten intermediate layer [J]. Diamond and Related Materials, 1995, 4(5/6): 754−758.

[9] BUIJNSTER J G, SHANKAR P, FLEISCHER W, ENCKEVORT W J P, SCHERMER J J, MEULEN J J. CVD diamond deposition on steel using arc-plated chromium nitride interlayers [J]. Diamond and Related Materials, 2002, 11(3/4/5/6): 536−544.

[10] LI Y S, TANG Y, YANG Q, XIAO C, HIROSE A. Diamond deposition on steel substrates with an Al interlayer [J]. International Journal of Refractory Metals & Hard Materials, 2009, 27(2): 417−420.

[11] KAWARADA M, KURIHARA K, SASAKI K. Diamond synthesis on a metal substrate [J]. Diamond and Related Materials, 1993, 2(5/6/7): 1083−1089.

[12] SILVA F J G,BAPTISTA A P M, PEREIRA E, TEIXEIRA V, FAN Q H, FERNANDE A J S, COSTA F M. Microwave plasma chemical vapour deposition diamond nucleation on ferrous substrates with Ti and Cr interlayers [J]. Diamond and Related Materials, 2002, 11(9): 1617−1622.

[13] POLINI R, MATTEI G, VALLE R, CASADEI F. Raman spectroscopy characterization of diamond films on steel substrates with titanium carbide arc-plated interlayer [J]. Thin Solid Films, 2006, 515(3): 1011−1016.

[14] WEI Qiu-ping, YU Zhi-ming, ASHFOLD M N R, MA Li, CHEN Zhong. Fretting wear and electrochemical corrosion of well-adhered CVD diamond films deposited on steel substrates with a WC-Co interlayer [J]. Diamond and Related Materials, 2010, 19(10): 1144−1152.

[15] WEI Qiu-ping, YU Zhi-ming, ASHFOLD M N R, CHEN Zhong, WANG Ling, MA Li. Effects of thickness and cycle parameters on fretting wear behavior of CVD diamond coatings on steel substrates [J]. Surface and Coatings Technology, 2010, 205(1): 158−167.

[16] WEI Qiu-ping, YU Zhing-ming, MA Li, YIN Deng-feng. Enhanced nucleation and smoothness of nanocrystalline diamond films via W-C gradient interlayer [J]. International Journal of Modern Physics B, 2009, 23(6/7): 1676−1682.

[17] WEI Qiu-ping, YU Zhi-ming, MA Li, YIN Deng-feng, YE J. The effects of temperature on nanocrystalline diamond films deposited on WC-13% Co substrate with W-C gradient layer [J]. Applied Surface Science, 2009, 256(5): 1322−1328. (in Chinese)

[18] WEI Qiu-ping, YU Zhing-ming, ASHFOLD M N R, YE J, MA Li. Synthesis of micro- or nano-crystalline diamond films on WC-Co substrates with various pretreatments by hot filament chemical vapor deposition [J]. Applied Surface Science, 2010, 256(13): 4357−4364. (in Chinese)

[19] WEI Qiu-ping, ASHFOLD M N R, MANKELEVICH Y A, YU Zhi-ming, LIU Pei-zhi, MA Li. Diamond growth on WC-Co substrates by hot filament chemical vapor deposition: Effect of filament-substrate separation [J]. Diamond and Related Materials, 2011, 20(516): 641−650.

[20] MAY P W, HARVEY J N, ALLAN N L, RICHLEY J C, MANKELEVICH Y A. Simulations of chemical vapor deposition diamond film growth using a kinetic Monte Carlo model [J]. Journal of Applied Physics, 2010, 108(1): 014905.

[21] CHERIAN K A, LITSTER J, RUDOLPH V, WHITE E T. Diamond needles and tips as engineered growth shapes [J]. Materials Research Society, 1996, 416: 241−247.

[22] FERRARI A C, ROBERTSON J. Origin of the 1 150 cm^{-1} Raman mode in nanocrystalline diamond [J]. Physical Review B, 2001, 63(12): 121405.

[23] SHRODER R E, NEMANICH R J, GLASS J T. Analysis of the composite structures in diamond thin films by Raman spectroscopy [J]. Physical Review B, 1990, 41(6): 3738.

[24] KLEIN C A, CARDINALE G F. Young's modulus and Poisson's ratio of CVD diamond [J]. Diamond and Related Materials, 1993, 2(5/6/7): 918.

[25] HUANG Zi-qian, HE Yue-hui, CAI Hai-tao, WU Cong-hai, XIAO Yi-feng, HUANG Bai-yun. Thermal residual stress analysis of diamond coating on graded cemented carbides [J]. Journal of Central South University of Technology: Science and Technology, 2008, 15(2): 165−169. (in Chinese)

[26] LIU H, DANDY D S. Studies on nucleation process in diamond CVD: An overview of recent developments [J]. Diamond and Related Materials, 1995, 4(10): 1173.

[27] POLINI R, MANTINI F P, BARLETTA M, VALLE R, CASADEI F. Hot filament chemical vapour deposition and wear resistance of diamond films on WC-Co substrates coated using PVD-arc deposition technique [J]. Diamond and Related Materials, 2006, 15(9): 1284−1291.

(Edited by HE Yun-bin)